

Influence of respiration on heart rate and blood pressure fluctuations

VERA NOVAK, PETER NOVAK, JACQUES DE CHAMPLAIN, A. ROBERT LE BLANC, RICHARD MARTIN, AND REGINALD NADEAU

Research Center, Hôpital du Sacré-Coeur de Montréal, and Departments of Physiology and Medicine and The Biomedical Engineering Institute, Faculty of Medicine, Université de Montréal, Montreal, Quebec H4J 1C5, Canada

NOVAK, VERA, PETER NOVAK, JACQUES DE CHAMPLAIN, A. ROBERT LE BLANC, RICHARD MARTIN, AND REGINALD NADEAU. *Influence of respiration on heart rate and blood pressure fluctuations*. *J. Appl. Physiol.* 74(2): 617–626, 1993.—The dynamics of the respiratory and cardiovascular systems were studied by continuously slowing respiration from 0.46 to 0.05 Hz. The time-frequency distribution and global spectral analysis were used to assess the R-R interval (R-R) and the systolic and diastolic blood pressure fluctuations in 16 healthy subjects. During rest, the nonrespiratory-to-respiratory frequency ratios were not affected by occasional slow breathing, whereas the low- (0.01–0.15 Hz) to high- (0.15–0.3 Hz) frequency indexes for blood pressure were increased ($P < 0.05$). The respiratory fluctuations in R-R and the systolic and diastolic pressures were paced over the 0.46- to 0.05-Hz range. As respiration slowed to 0.07–0.09 Hz, the frequency content of the respiration and cardiovascular variables increased sharply and nonlinearly to a maximum that exceeded values at higher frequencies ($P < 0.001$). The nonrespiratory frequency content remained stable in the 0.01- to 0.05-Hz range and did not significantly differ from that at rest. In contrast, the nonstable 0.05- to 0.1-Hz component was suppressed. A slow 0.012- to 0.017-Hz rhythm modulated respiration and hemodynamic fluctuations at both respiratory and nonrespiratory frequencies. The study indicated that respiration input should be considered in the interpretation of global spectra. Furthermore the time-frequency distributions demonstrated that a close nonlinear coupling exists between the respiratory and cardiovascular systems.

slowing of respiration; R-R interval; blood pressure; spectral estimation

FLUCTUATIONS IN CONSECUTIVE QRS complexes (R-R) are known as respiratory sinus arrhythmia and are recognized as a measure of parasympathetic tone (13). They are usually evaluated in a narrow band (0.15–0.30 Hz), regardless of the fact that the frequencies of spontaneous respiration can spread over a wider range (2). By controlling respiration at discrete frequencies, it has been shown that, between 0.06 and 0.5 Hz, these fluctuations are transferred to the R-R interval (31, 35). The amplitude of the R-R fluctuations is proportional to the tidal volume, and, for a given tidal volume, it increases as the respiratory frequency slows (2, 5, 13, 29). Several authors attempted to identify spectral peaks in predefined ranges (low frequencies 0.01–0.05 Hz and 0.05–0.15 Hz, high frequencies 0.15–0.3 Hz) that might be associated with the

renin-angiotensin, thermoregulatory, sympathetic, or parasympathetic systems (16, 19). However, assessment of the autonomic nervous system, on the basis of the powers within these ranges and the ratios of low to high frequency, has not always been successful (32). Only parasympathetic muscarinic blockade consistently suppresses R-R fluctuations over the whole range from 0.01 to 0.4 Hz. The effect of the sympathetic blockade remains ambiguous (1, 34). The enhancement of the R-R and blood pressure fluctuations at low frequencies could originate from the decrease of the mean vagal as well as sympathetic tones (4). Furthermore, heart rate and blood pressure fluctuations were observed concomitantly with the periodic tidal volume changes (0.01–0.03 Hz) that occurred in adults and newborns during sleep (9, 12, 14). Thus it is difficult to directly relate the specific spectral peaks to the sympathetic or parasympathetic tones.

In this study, the coupling between the respiratory and cardiovascular systems was evaluated by continuously slowing respiration over the 0.46- to 0.05-Hz range.

METHODS

Subjects. Fourteen male and two female (aged 23–37 yr) healthy subjects participated in the study. No subject had a history of cardiopulmonary disease. All the experiments were done in a light-attenuated room between 9 A.M. and 3 P.M. with the subject in a supine position.

Data acquisition. The respiration signal (by a nasal thermistor), electrocardiogram (lead II), and noninvasive beat-to-beat blood pressure from the third finger (by photoplethysmographic transducer, Ohmeda Finapres) (6) were recorded. Continuous data acquisition for each experimental condition was done at a sampling rate of 200 samples/s. This sampling rate was adequate to maintain the accuracy of the R wave, systolic (SBP) and diastolic blood pressure (DBP) detection algorithms, fiducial marking, and time interval measurements. R-R was detected as intervals between consecutive R waves of the QRS complexes of the electrocardiograms. Signals were acquired and stored on a personal computer-based system equipped with an eight-channel analog-to-digital acquisition card (Data Translation model DT 2801).

Technique of respiration. The subjects were instructed to inhale-exhale in synchrony with each tone in a sequence of 100-ms beeps recorded on a cassette tape. The cassette was replayed for each recording session. By

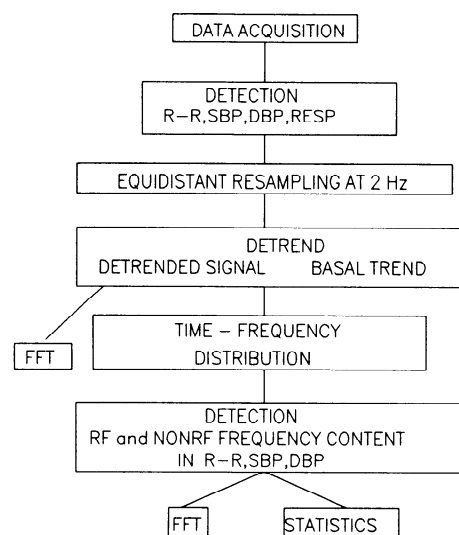


FIG. 1. Computing procedures. Data acquisition is followed by detection of R-R intervals (R-R), systolic (SBP) and diastolic blood pressures (DBP), and respiration (RESP). Time-frequency distributions and global spectra (fast Fourier transform, FFT) are computed after removal of baseline trend. Respiratory (RF) and nonrespiratory (NONRF) frequency contents are detected on time-frequency distributions and evaluated again by FFT in determination of amplitude modulation rhythm.

lengthening the respiratory period from 2.17 to 20 s within an 8.5-min interval, a continuous slowing of the respiratory rate from 0.46 to 0.05 Hz was achieved.

Experimental protocol. All the subjects gave their signed consent. Spontaneous respiration was monitored for 10 min during rest in the supine position before synchronized respiration was begun. Tidal volume was not controlled, and subjects were allowed to breathe comfortably to allow for adjustments to the acid-base balance.

Data processing, computing, and statistical analysis. R-R, SBP and DBP, and respiratory values were obtained from the electrocardiogram, blood pressure, and respiratory signals (Fig. 1). Because interpolated time series were required for spectral estimations, these values were linearly interpolated at 2 Hz to ensure equidistant sampling in each time series. A moving fourth-order polynomial function (a nonlinear band-pass filter) was used to remove the baseline trend from all the signals. This filtering excluded the very-low-frequency nonstationarity (<0.005 Hz) but did not affect the higher frequencies. In RESULTS, this trend is referred to as the basal trend of R-R and blood pressure.

The beat-to-beat spectral estimation analysis was

based on the discrete Wigner distribution (8, 30, 37). The Wigner distribution, which decomposes a signal into a function of time and frequency, has been shown to be a good method for estimating a short nonstationary time series (26). Its high resolution was achieved by independent time and frequency smoothing by use of a moving 128-event data window. The time-frequency distributions were computed with the same parameter set for all the signals. In addition, the cross time-frequency distributions were calculated to show common frequency contents among respiration, R-R, and blood pressure (for details of the adaptation of the method to these signals, see APPENDIX).

The frequency contents were classified as respiratory and nonrespiratory for each time instant (Fig. 2A). The respiratory frequency content was defined as the local maximum at the actual respiratory frequency on the respiratory, R-R, SBP, and DBP time-frequency distributions. The remaining nonrespiratory frequency content was identified as the local maximum at frequencies ranging from the respiratory frequency down to 0.01 Hz. The trends of the frequency content at respiratory frequencies were correlated with the frequency content of respiration. During synchronized respiration, the R-R interval and SBP trends between 0.1 and 0.46 Hz were approximated by linear regression.

Additionally, initial interpolated and detrended time series for the resting periods were analyzed by a single Fourier transform [with use of the fast Fourier algorithm (FFT) (27)] of the entire time series. This is referred to as the global spectrum. Spectral powers were averaged across the low- (0.01–0.15 Hz) and high-frequency (0.15–0.3 Hz) ranges. The ratios of low to high frequency were computed and averaged across the population.

The amplitude modulations of the respiratory and nonrespiratory frequency contents were evaluated by computing the global spectrum from the beat-to-beat respiratory and nonrespiratory frequency contents during the resting and synchronized respiration. Student's paired *t* test was used to compare the amplitudes of the dominant peaks.

Student's paired *t* test was also used for the group comparisons of the nonrespiratory and respiratory frequency contents of the low and high frequencies and their ratio during the resting periods.

RESULTS

Resting—spontaneous respiration. The beat-to-beat dynamics of the cardiovascular fluctuations are shown on

TABLE 1. Averaged powers from time-frequency distributions compared with global spectra at rest

	Time-Frequency Distributions			Global Spectra		
	RF	NONRF	NONRF/RF	HF	LF	LF/HF
R-R, ms ² /Hz	2,293.6±87.9	2,736.1±476.5	1.19±5.5	9,984±989.3	15,846.8±7,327.6	4.4±1.8
SBP, mmHg ² /Hz	7.7±1.1	34.3±9.6*	4.45±3.7	13.4±4.5	164.1±28.4*	18.6±3.4†
DBP, mmHg ² /Hz	2.9±0.2	10.3±0.6*	3.35±3.0	4.1±4.8	52.7±12.2*	19.1±4.6†

Values are means ± SE; *n* = 16. R-R, R-R interval; SBP, systolic pressure; DBP, diastolic pressure; RF, respiratory frequencies; NONRF, nonrespiratory frequencies; HF, high frequencies (0.15–0.3 Hz); LF, low frequencies (0.01–0.15 Hz). * NONRF vs. RF in time-frequency distributions and LF vs. HF in global spectra (*P* < 0.05). † NONRF/RF vs. LF/HF indexes (*P* < 0.05).

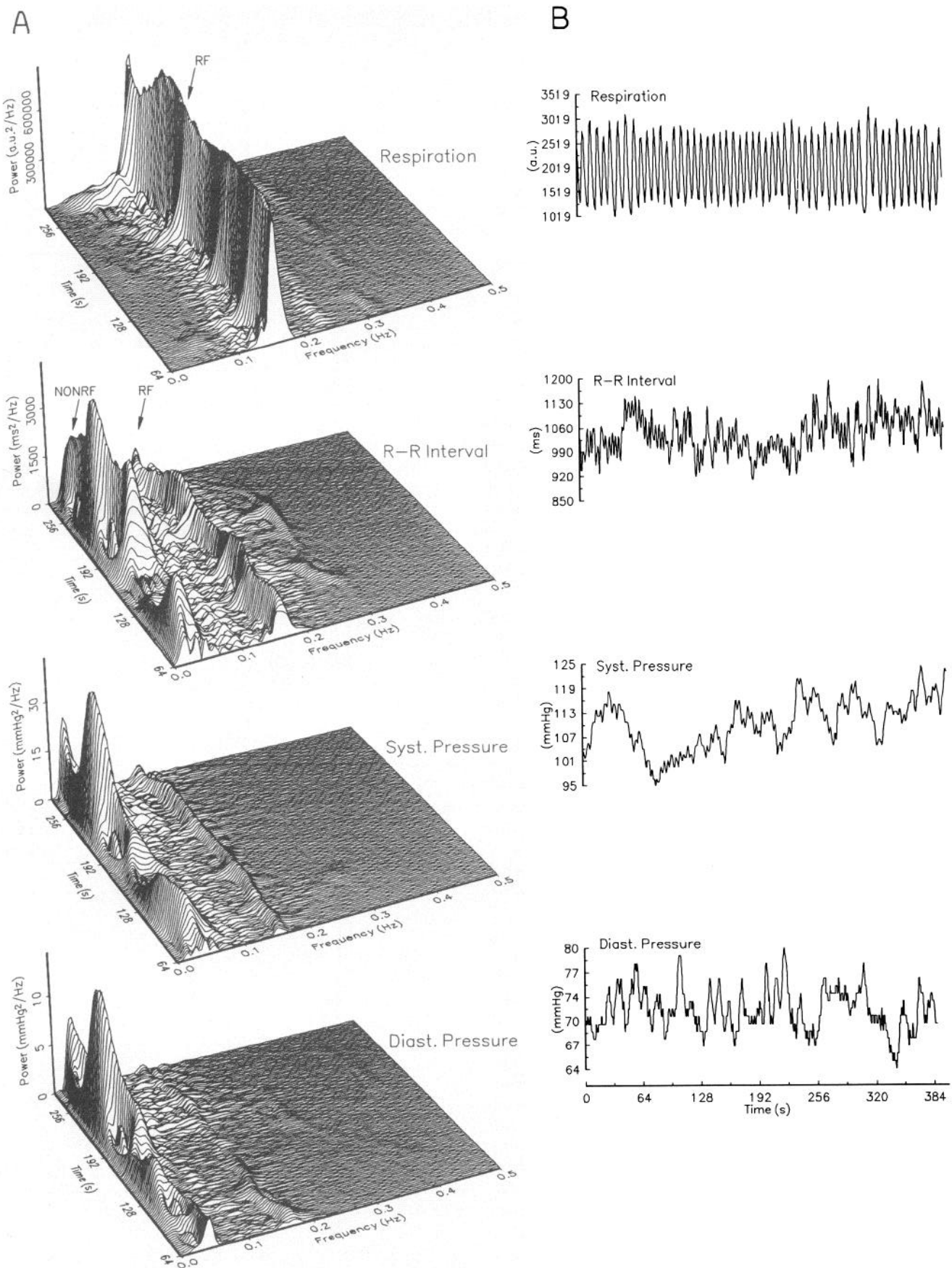


FIG. 2. Example of regular spontaneous respiration at rest (subj 1). A: time-frequency distributions of respiration, R-R interval, and systolic and diastolic pressures with respiratory (RF) and nonrespiratory frequency (NONRF) content noted. B: signals of respiration, R-R, and systolic and diastolic pressures. Respiratory frequency content is localized at 0.15 Hz and nonrespiratory frequency at ~ 0.03 Hz.

the time-frequency distribution charts (Fig. 2). The respiratory and nonrespiratory frequency contents are clearly identifiable and continuously present. When respiration was regular, the respiratory frequency contents of R-R, SBP, and DBP were concentrated in a narrow band around its dominant frequency (mean 0.19 Hz, range 0.1–0.23 Hz). Any changes in the dominant frequency were reflected in the respiratory fluctuations. In the global spectrum of respiration, this dominant frequency appeared as the main peak (Fig. 3). Corresponding peaks were identified in the R-R and SBP and smaller peaks in DBP.

The nonrespiratory spectral content was continuously detectable in the 0.01- to 0.05-Hz range, and it was relatively stable around 0.02–0.03 Hz (Fig. 2). Accordingly, the global spectra have shown the dominant peak at low frequencies (Fig. 3). In contrast, the range between 0.05 Hz and the respiratory frequency was unstable, and the frequency content increased only occasionally. This component tended to arise when the nonrespiratory frequency content at lower frequencies had higher amplitude or spread above 0.05 Hz (Fig. 2). During rest the nonrespiratory fluctuations in SBP and DBP were higher ($P < 0.05$) than the respiratory fluctuations. Furthermore the mean powers from the global spectra at the low (0.01–0.15 Hz) frequencies were higher ($P < 0.05$) than at the high (0.15–0.30 Hz) frequencies in both SBP and DBP (Table 1).

In some cases, spontaneous respiration was not regular and the dominant frequency was affected by the slower breathing (Fig. 4). This generally occurred at 0.1 Hz and occasionally as low as 0.02 Hz. Cross time-frequency distributions confirmed that such respiratory patterns were directly transferred to R-R, SBP, and DBP at the corresponding frequencies. Thus, these slow breaths caused an immediate increase in the frequency content and appeared as peaks on the low frequencies, where respiratory influence is rarely expected. Accordingly, the global spectrum showed a peak at the same frequency.

The ratios of low to high frequencies from the global spectra were elevated ($P < 0.05$) over nonrespiratory/respiratory frequency content indexes in both SBP and DBP (Table 1). Thus the higher values of the global spectra indexes were false positive. Because occasional slowing of the respiratory frequency below 0.15 Hz can affect the powers in the lower range, the respiratory frequency contents at low frequencies should be carefully excluded. The resting values were R-R, 903 ± 3.6 (SE) ms; SBP, 127.6 ± 0.3 mmHg; and DBP, 64.6 ± 0.2 mmHg.

Synchronized respiration. Time-frequency distributions have clearly shown that breath-to-breath slowing of respiration from 0.46 to 0.05 Hz continuously paced the respiratory fluctuations in R-R, SBP, and DBP over the entire range (Fig. 5). The beat-to-beat respiratory frequency contents were averaged across subjects for each time instant (Fig. 6A). The respiratory frequency content, which increased nonlinearly and inversely to the frequency of breathing, reached its maximum at 0.07–0.09 Hz. The R-R, SBP, and DBP respiratory frequency contents rose in parallel and reached their maximum at

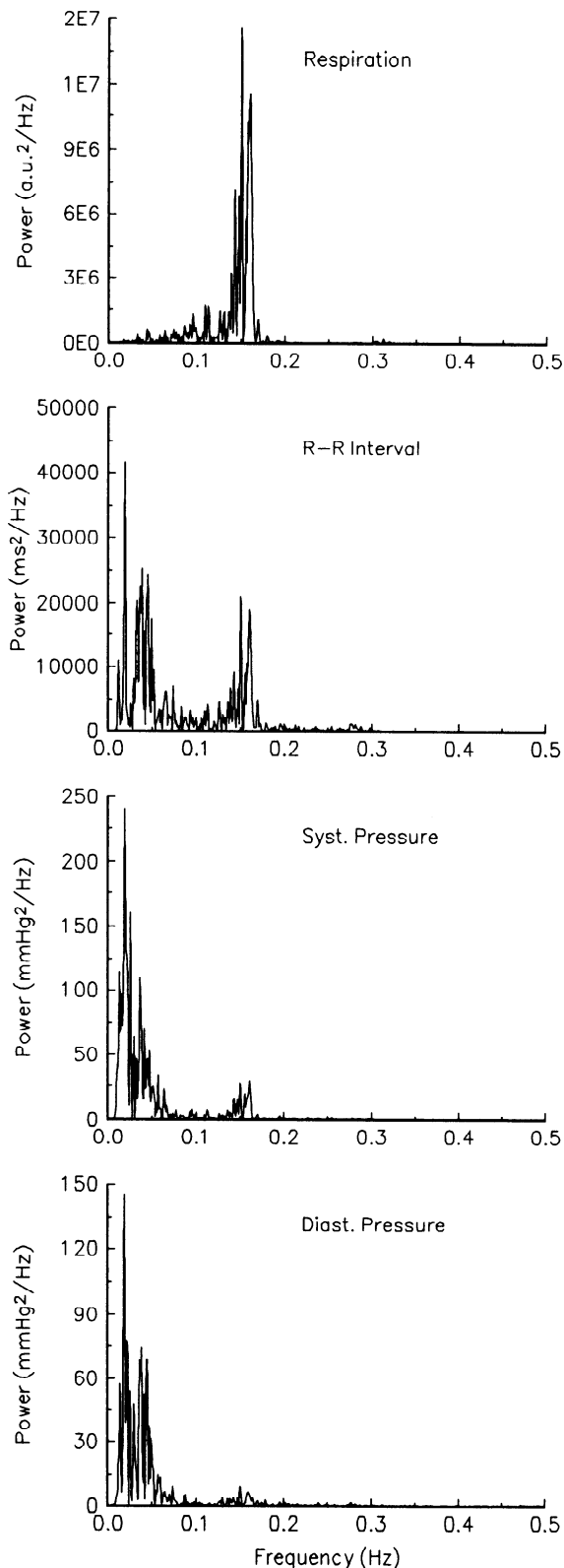


FIG. 3. Global FFT power spectra of signals from Fig. 2. Two main peaks at respiratory (0.15 Hz) and nonrespiratory (0.03 Hz) frequencies can be identified in R-R interval and systolic and diastolic pressures.

the same time ($r = 0.99$, 0.827, and 0.76, respectively). The maximal values [R-R frequency 0.07 Hz, $13,576 \pm 246$ (SE) ms^2/Hz ; SBP frequency 0.09 Hz, 63.8 ± 3.1

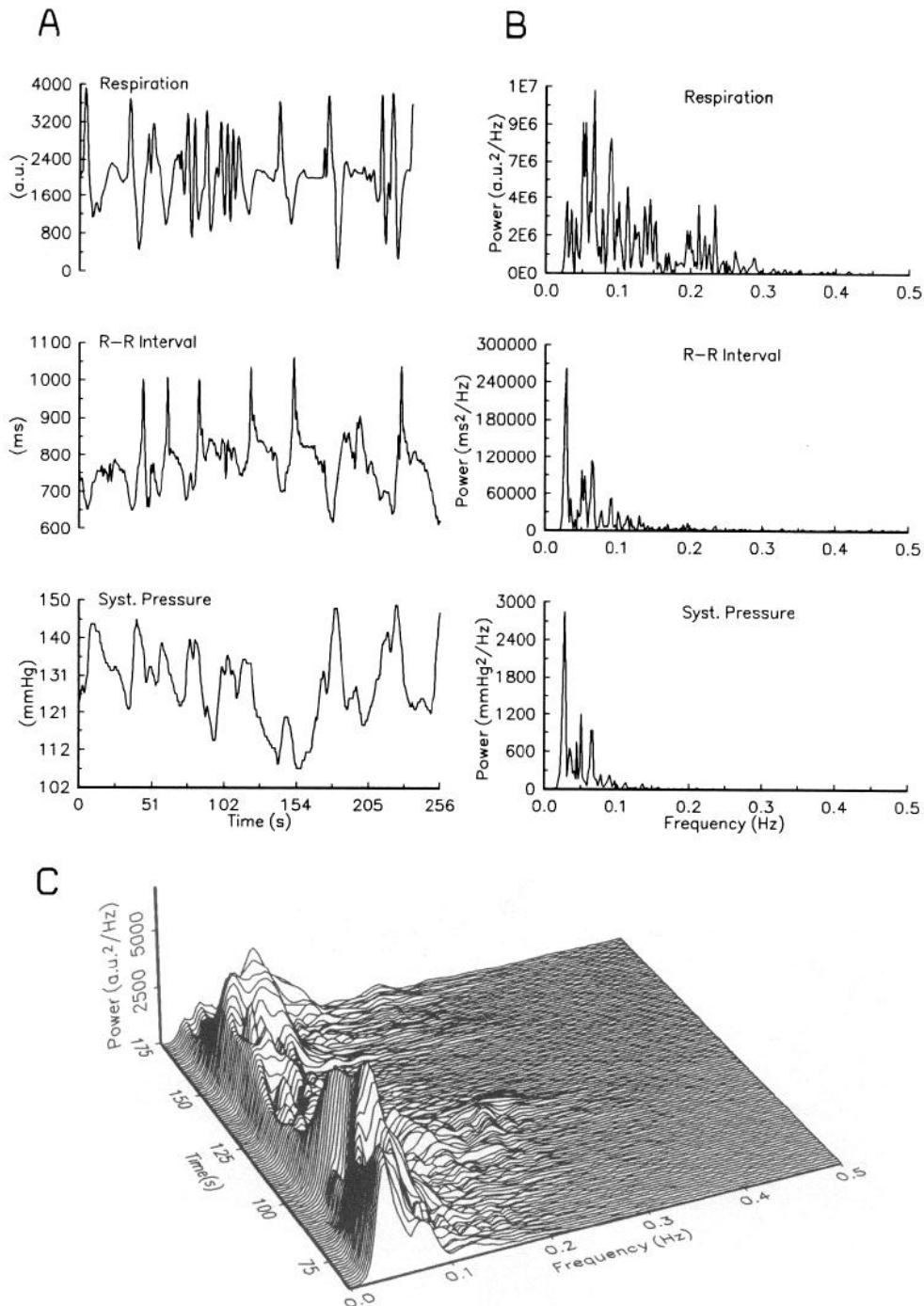


FIG. 4. Example of increase in frequency content caused by an irregular respiratory pattern (faster respiratory frequency is mixed with slow breaths and short apneas) at low frequencies. **A:** signals of respiration, R-R intervals, and systolic pressure at rest (*subj 2*). **B:** global power spectra. **C:** cross time-frequency distribution between respiration and systolic blood pressure showing transfer of low-frequency respiration pattern to systolic pressure.

mmHg²/Hz; DBP frequency 0.09 Hz, 21.33 ± 2.3 mmHg²/Hz; $P < 0.001$] greatly exceeded the resting values, whereas the values at 0.19 Hz corresponded to the mean of those at the resting respiratory frequency.

The nonrespiratory frequency contents of the three variables remained unaffected in the 0.02- to 0.03-Hz range and did not significantly differ from those at rest. The highly nonstable nonrespiratory component around 0.1 Hz was almost completely suppressed when respiration was paced at the higher frequencies. However, when slowed to 0.07 Hz, it synchronized with respiration. The baseline trend was also computed as an average across the population for each time index. The R-R and SBP

baseline trends decreased ($P < 0.05$) as the respiratory frequency decreased (Fig. 6B), whereas the DBP trend remained unchanged.

Amplitude modulation. The time-frequency distributions revealed that the crests of the respiratory and nonrespiratory frequency contents are modulated by a slower rhythm, which was present both at rest (Fig. 2) and during synchronized respiration (Fig. 5). Subsequent FFT spectra have detected its dominant frequency at 0.012–0.017 Hz in respiration, R-R, SBP, and DBP at both respiratory and nonrespiratory frequencies. The dominant peaks were significantly higher (R-R, $P < 0.001$; SBP and DBP, $P < 0.05$) during the synchronized

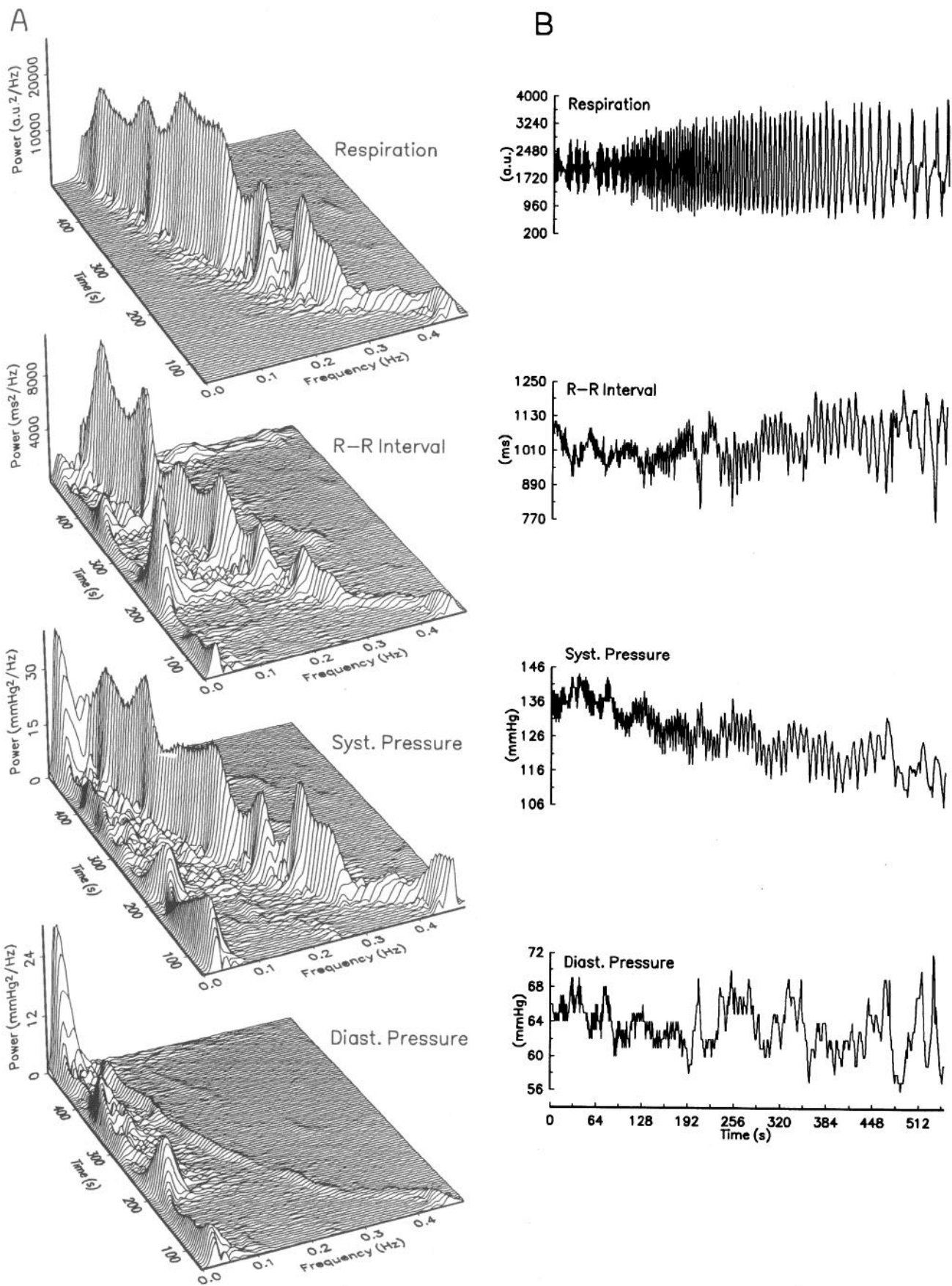


FIG. 5. A: time-frequency distributions of respiration, R-R intervals, and systolic and diastolic pressures. B: signals during continuous slowing of respiration (*subj 3*). Frequency contents in all signals continuously follow respiratory frequencies between 0.46 and 0.05 Hz. Respiratory amplitude modulation is apparent in all signals at both respiratory and nonrespiratory frequencies.

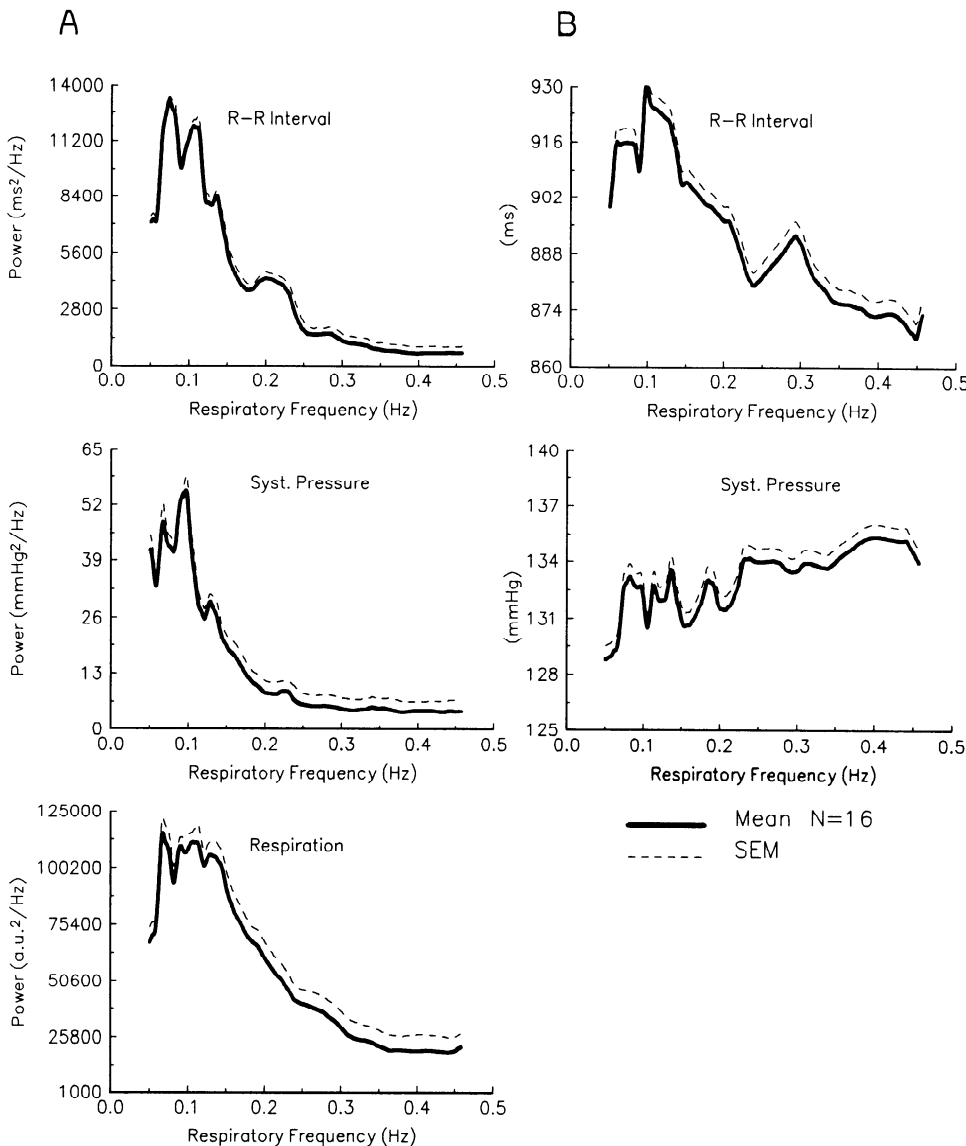


FIG. 6. A: powers of respiration, R-R intervals, and systolic pressure at respiratory frequencies during synchronized respiration plotted against corresponding respiratory frequencies from 0.46 Hz (time = 0 s) to 0.05 Hz (time = 480 s). B: average basal trend of R-R intervals and systolic pressure with respect to corresponding respiratory frequencies during synchronized respiration.

respiration than during rest at respiratory frequencies (Fig. 7). The peaks at nonrespiratory frequencies during synchronized respiration did not differ from those during rest (R-R, $215,995 \pm 10,032 \text{ ms}^4/\text{Hz} \times 10^4$; SBP, $16,315.5 \pm 3,182.3 \text{ mmHg}^4/\text{Hz}$) but were lower in DBP (rest, $3,402.2 \pm 573.3 \text{ mmHg}^4/\text{Hz}$; synchronized respiration, $2,180.5 \pm 22.5 \text{ mmHg}^4/\text{Hz}$).

DISCUSSION

Our results indicate that respiration can override the hemodynamic fluctuations in both the time and frequency domains. In recently proposed single input-single output models, respiration is considered to be an input for the sinoatrial node and baroreflex loops. The system dynamics are assumed to be linear for small perturbations around a given operating point, but not from one operating point to another (11, 36). The respiratory input, which increased nonlinearly toward the low frequencies, was accompanied by a parallel output in the cardiovascular variables. Thus the degree of coupling is relatively independent of respiratory frequency in the

range shown. During breathing at low frequencies, where large lung volumes can be expected (2, 5, 8, 13), the respiratory R-R fluctuations are increased secondary to the afferent feedback from the pulmonary slowly adapting and stretch receptors (10). However, the blood pressure fluctuations tend toward a greater reflection of the effects of the intrathoracic inspiratory-expiratory mechanics on the venous return and, in turn, on cardiac output.

Attempts have been made to associate the R-R and blood pressure fluctuations in the 0.05- to 0.1-Hz range with the baroreflex or sympathetic tone indexes (1, 16). However, our study has clearly demonstrated that the nonrespiratory spectral content in this range is unstable and can be altered easily. It is suppressed by pacing respiration at higher frequencies and increased by pacing at lower frequencies. At rest, the spontaneous slowing of respiration to the lower range is common, and consequently frequency content is enhanced. The respiratory input in the 0.05- to 0.1-Hz range is high, and therefore the corresponding hemodynamic fluctuations greatly exceed the resting values. Consequently, if the respiratory

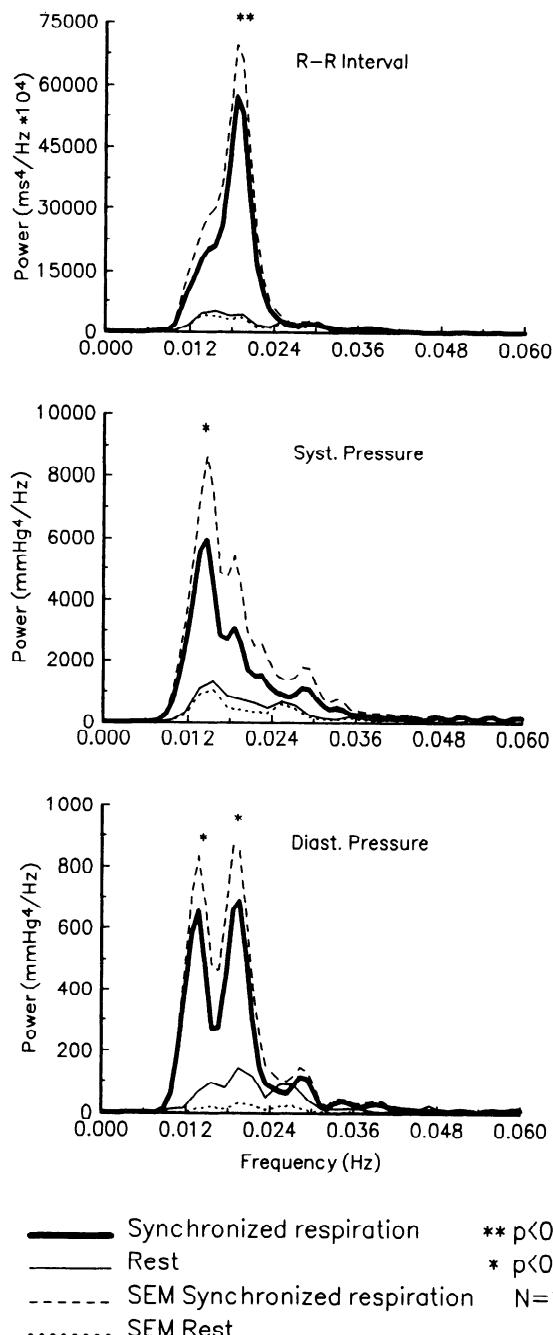


FIG. 7. Average global spectra from amplitude modulation at respiratory frequencies of R-R intervals and systolic and diastolic pressures at rest and during synchronized respiration. SEM, standard error of mean.

spectral content in this range is not extracted, or if respiration is not considered, the indexes based on the ratio of low to high frequency can be artificially elevated. Thus, false positive results may be obtained if they are used as markers of sympathoexcitation in pathologies (18, 22) where alteration of respiratory patterns can occur.

The nonrespiratory frequency content in the 0.01- to 0.05-Hz range was continuously detectable both at rest and during synchronized respiration. The respiratory influence on R-R interval fluctuations in the 0.01- to 0.05-Hz range has been associated with tidal volume changes and is considered to be a sign of instability of the ventila-

tory chemoreceptor feedback mechanisms (7, 20, 28). Because the intrathoracic pressure changes are relatively low, the direct mechanical transfer of tidal volume oscillations to the heart rate and blood pressure fluctuations was not taken into consideration (3, 14). However, this study confirms that the 0.012- to 0.017-Hz rhythm modulates the amplitude of the R-R and blood pressure fluctuations at both respiratory and nonrespiratory frequencies. The power of the amplitude modulation increased at respiratory frequencies during synchronized respiration. Although this could be simply a multiplicative phenomenon, i.e., the depth of the modulation is greater when the signal is greater, it nevertheless demonstrates a strengthening of the coupling between the two systems. Animal studies have shown synchronization among reticular-respiratory-neuron discharges (21, 23), undulating breathing patterns, phrenic and sympathetic bursts (17, 31, 33), and blood pressure fluctuations at similar frequencies. Recently the 0.02- and 0.05-Hz rhythms were found to modulate the basal electroencephalographic activity (24, 25). We suggest that the 0.012- to 0.017-Hz rhythm, which modulates the amplitude of respiration, R-R, and blood pressure fluctuations, reflects the presence of the brain stem network common to cardiovascular and respiratory systems.

Continuous slowing of respiration frequency has clearly demonstrated that respiration can pace the hemodynamic fluctuations and that both systems are modulated by the same rhythm. Moreover, a multifactorial nonlinear coupling among the respiratory, the cardiovascular, and the autonomic nervous system was illustrated.

APPENDIX

The application to cardiovascular signals of the modified Wigner distributions for the derivation of time-frequency distributions from spectral estimations has been developed by Novak and Lepicovska (26) and has proven to be a good estimation method for a short and nonstationary time series. A proper parameter set has been determined experimentally and uniformly applied to all the respiration and cardiovascular signals.

The function used to calculate the modified Wigner distribution is

$$W_{zx}(n, m) = \frac{1}{2}N \sum_{k=0}^{N-1} |h(k)|^2 \\ \times \sum_{p=-M+1}^{M-1} g(p)z(n+p+k)x^*(n+p-k)e^{-2i\pi km/N} \quad (1)$$

where n is the time index, m is the frequency index, $h(k)$ and $g(p)$ are frequency and time smoothing windows (15), respectively (both are presented more thoroughly below), N is the time window over which a spectral estimation is calculated, and M is the parameter defining the time smoothing window width. It has been noted that the time window is much shorter than N and is centered at the actual time index, n .

For our specific application, interpolated and detrended data from each time series are used for the calculations. To apply Eq. 1, each time series needs to be transformed into an analytic signal in which the real part is the interpolated and detrended signal and the imaginary part is the same signal with a 90° shift. The Hilbert transform (26) was used for this conversion. For a given time series, it establishes the z analytic signal of Eq. 1. For another time series, the same transformation will estab-

lish the x analytic signal. When two different time series are used for the calculation, the result is the cross time-frequency distribution. If we use the same time series (i.e., if $z = x$), the result will be the auto time-frequency distribution or simply time-frequency distribution.

The Wigner distribution of the analytic signal has been shown to eliminate the interference between positive and negative frequencies as well as the occurrence of spurious peaks. However, further suppression of spurious peaks is achieved by using independent time and frequency smoothing. Time smoothing uses a rectangular window $g(p)$, which is $2M - 1$ samples wide ($M = 9$ has been determined experimentally as the most appropriate)

$$h(k) = e^{-1/2[\alpha k/(N/2)]^2} \quad 0 \leq |k| \leq N/2 \\ 2.5 \leq \alpha \leq 3.5 \quad (2)$$

The time-frequency distributions (auto and cross) were calculated with the same parameter set for all the signals: data window $N = 128$ samples; smoothing window $M = 9$ samples; $h(k)$ is Gaussian window, which is $N - 1$ wide, where $\alpha = 2.8$; and $g(p) = 1$, a unit rectangular window.

With these parameters, it has been possible to generate reliable estimates of time-frequency distributions that follow the signal structure particularly well in nonstationary conditions. Moreover, they have allowed a better evaluation of the frequency content of transitory periods that cannot be obtained otherwise. The program for time-frequency distribution calculations was written in C++ and implemented on a personal computer (80386/80387, 33 MHz) running under MS-DOS.

Address for reprint requests: V. Novak, Dept. of Neurology, Jewish General and Sir Mortimer B. Davis Hospital, McGill University, 3755 Chemin de la Côte St. Catherine, Montreal, Quebec H3T 1E2, Canada.

Received 8 August 1991; accepted in final form 11 September 1992.

REFERENCES

- AKSELROD, S., D. GORDON, J. B. MADWED, N. C. SNIDMAN, D. C. SHANNON, AND R. J. COHEN. Hemodynamic regulation: investigation by spectral analysis. *Am. J. Physiol.* 249 (Heart Circ. Physiol. 18): H867-H875, 1985.
- ANGELONE, A., AND N. A. COULTER. Respiratory sinus arrhythmia: a frequency dependent phenomenon. *J. Appl. Physiol.* 19: 479-482, 1964.
- APPEL, M. L., J. P. SAUL, R. D. BERGER, AND R. J. COHEN. Closed-loop identification of cardiovascular regulatory mechanisms. *Proc. Comp. Cardiol. Jerusalem* 1989, p. 19-22.
- BERGER, R. D., J. P. SAUL, AND R. J. COHEN. Transfer function analysis of autonomic regulation. I. Canine atrial response. *Am. J. Physiol.* 256 (Heart Circ. Physiol. 25): H142-H152, 1989.
- BERNARDI, C., F. KELLER, M. SANDERS, P. S. REDDY, B. GRIFFITH, F. MENO, AND M. R. PINSKY. Respiratory sinus arrhythmia in the denervated human heart. *J. Appl. Physiol.* 67: 1447-1455, 1989.
- BOEHMER, R. D. Continuous, real-time, noninvasive monitor of blood pressure: Penaz methodology applied to the finger. *J. Clin. Monit.* 3: 282-287, 1987.
- BROWN, H. W., AND F. PLUM. The neurological basis of Cheyne Stokes respiration. *Am. J. Med.* 30: 849-860, 1961.
- CLAASEN, T. A. C. M., AND W. F. G. MECKLENBRAUKER. The Wigner distribution—a tool for time frequency signal analysis. I. Continuous-time signals. *Philips J. Res.* 35: 217-250, 1980.
- COCCAGNA, G., M. MANTOVANI, F. BRIGNANI, A. MANZINI, AND E. LUGARESIS. Arterial pressure changes during spontaneous sleep in man. *Electroencephalogr. Clin. Neurophysiol.* 31: 277-281, 1971.
- DALY, M. B., AND E. KIRKMAN. Differential modulation by pulmonary stretch afferents of some reflex cardioinhibitory responses in the cat. *J. Physiol. Lond.* 417: 323-341, 1989.
- DE BOER R. W., J. W. KAREMAKER, AND J. STRACKEE. Hemodynamic fluctuations and baroreflex sensitivity in humans: a beat-to-beat model. *Am. J. Physiol.* 253 (Heart Circ. Physiol. 22): H680-H689, 1987.
- DYKES, F. D., P. A. AHMANN, K. BALDZER, T. CARRIGAN, R. KITNEY, AND D. P. GIDDENS. Breath amplitude modulation of heart rate variability in normal full term neonates. *Pediatr. Res.* 20: 301-308, 1986.
- ECKBERG, D. L. Human sinus arrhythmia as an index of vagal cardiac outflow. *J. Appl. Physiol.* 54: 961-966, 1983.
- GIDDENS, D. P., AND R. I. KITNEY. Neonatal heart rate variability and its relations to respiration. *J. Theor. Biol.* 113: 759-780, 1985.
- HARIS, F. J. On the use of windows for harmonic analysis with the discrete Fourier transform. *Proc. IEEE* 66: 51-83, 1978.
- HAYANO, J., Y. SAKAKIBARA, M. YAMADA, T. KAMIYA, T. FUJINAMI, K. YOKO-YAMA, Y. WATANABE, AND K. TAKATA. Diurnal variations in vagal and sympathetic cardiac control. *Am. J. Physiol.* 258 (Heart Circ. Physiol. 27): H642-H646, 1990.
- HUKUHARA, T. Discharge properties of respiratory modulated brainstem reticular neurons, and their relation to slow arterial pressure fluctuations in rabbit. In: *Mechanisms of Blood Pressure Waves*, edited by K. Miyakawa, H. P. Koepchen, and C. Polosa. Berlin: Springer-Verlag, 1984, p. 241-254.
- KIENZLE, M. G., D. W. FERGUSSON, C. L. BIRKETT, G. A. MYERS, W. J. BERG, AND J. MARIANO. Clinical, hemodynamic and sympathetic neural correlates of heart variability in congestive heart failure. *Am. J. Cardiol.* 69: 761-767, 1992.
- KITNEY, R. I. An analysis of the nonlinear behaviour of the human thermal vasomotor control system. *J. Theor. Biol.* 52: 231-248, 1975.
- LANGE, R. L., AND H. H. HECHT. The mechanisms of Cheyne-Stokes respiration. *J. Clin. Invest.* 41: 41-52, 1962.
- LANGHORST, P., G. SCHULTZ, M. LAMBERTZ, AND H. MANERE. Dynamic characteristic of the "unspecific brain stem system." In: *Central Interaction Between Respiratory and Cardiovascular Control Systems*, edited by H. P. Koepchen, S. M. Hilton, and A. Trzebski. Berlin: Springer-Verlag, 1980, p. 30-39.
- MALLIANI, A., M. PAGANI, F. LOMBARDI, R. FURLAN, S. GUZZETTI, AND S. CERUTTI. Spectral analysis to assess increased sympathetic tone in arterial hypertension. *Hypertension Dallas* 17, Suppl. III: III-36-III-42, 1991.
- MIYAKAWA, K., T. TADEUCHI, AND T. SHIMIZU. Mechanisms of blood pressure waves of the third order. In: *Neural Mechanisms and Cardiovascular Disease*, edited by B. Lown, A. Malliani, and M. Pordescimi. Padua, Italy: Liviana, 1986, p. 291-302.
- NOVAK, P., AND V. LEPOCOVSKA. Slow modulation of EEG. *Neuroreport* 3: 189-192, 1992.
- NOVAK, P., V. LEPOCOVSKA, AND C. DOSTALEK. Periodic amplitude modulation of EEG. *Neurosci. Lett.* 13: 213-215, 1992.
- NOVAK, P., AND V. LEPOCOVSKA. Time-frequency mapping of the heart rate, blood pressure and respiratory signals. *Med. Biol. Eng. Comput.* In press.
- OPPENHEIM, A. V., AND R. W. SCHAFER. *Digital Signal Processing*. Englewood Cliffs, NJ: Prentice-Hall, 1985, p. 532-562.
- PACK, A. I., D. SILAGE, R. P. MILLMAN, H. KNIGHT, E. T. SHORE, AND D. C. CHUNG. Spectral analysis of ventilation in elderly subjects awake and asleep. *J. Appl. Physiol.* 64: 1257-1267, 1988.
- PAGANI, M., F. LOMBARDI, S. GUZZETTI, O. RIMIDI, R. FURLAN, P. PIZZINELLI, G. SANDRONE, G. MALFATTO, S. DELL'ORTO, E. PICCALUGA, M. TURIEL, G. BASELLI, S. CERUTTI, AND A. MALLIANI. Power spectral analysis of heart rate and arterial pressure variabilities as a marker of sympatho-vagal interaction in man and conscious dog. *Circ. Res.* 59: 178-193, 1986.
- PEYRIN, F., AND R. PROST. A unified definition for the discrete-time, discrete frequency and discrete time/frequency Wigner distributions. *IEEE Trans. Acoustic Speech Signal Processing* 34: 859-867, 1986.
- POLOSA, C. Haemorrhage and blood pressure waves. In: *Mechanisms of Blood Pressure Waves*, edited by K. Miyakawa, H. P. Koepchen, and C. Polosa. Berlin: Springer-Verlag, 1984, p. 147-166.
- POMERANZ, B., R. J. B. MACAULAY, M. A. CAUDILL, I. KUTZ, D. ADAM, D. GORDON, K. M. KILBORN, A. C. BARGER, D. C. SHANNON, R. J. COHEN, AND H. BENSON. Assessment of autonomic function in humans by heart rate spectral analysis. *Am. J. Physiol.* 248 (Heart Circ. Physiol. 17): H151-H153, 1985.

33. PREIS, G., AND C. POLOSA. Patterns of sympathetic neuron activity associated with Mayer waves. *Am. J. Physiol.* 226: 724-730, 1974.
34. RANDALL, D. C., D. R. BROWN, R. M. RAISCH, J. D. YINGLING, AND W. C. RANDALL. SA nodal parasympathectomy delineates autonomic control of heart rate power spectrum. *Am. J. Physiol.* 260 (*Heart Circ. Physiol.* 29): H985-H988, 1991.
35. SAUL, J. P., R. D. BERGER, M. H. CHEN, AND R. J. COHEN. Transfer function analysis of autonomic regulation. II. Respiratory sinus arrhythmia. *Am. J. Physiol.* 256 (*Heart Circ. Physiol.* 25): H153-H161, 1989.
36. SAUL, J. P., R. D. BERGER, AND R. J. COHEN. Short term blood pressure regulation: a combination of feedback and mechanics (Abstract). *Proc. Annu. Int. Conf. IEEE Eng. Med. Biol. Soc.* 12: 2, 1990.
37. WIGNER, E. P. On the quantum correction for thermodynamic equilibrium. *Physical Rev.* 40: 749-759, 1932.

